

# Finite Element Modeling of Electric Field Effects of TASER Devices on Nerve and Muscle

Dorin Panescu, Ph.D.\*, Mark W. Kroll, Ph.D.\*\*, Igor R. Efimov, Ph.D.\*\*\* and James D. Sweeney, Ph.D.\*\*\*\*

\* - St. Jude Medical, Sunnyvale, CA, \*\* - Cal Poly University, San Luis Obispo, CA, \*\*\* - Washington University, St. Louis, MO, \*\*\*\* - Arizona State University, Phoenix, AZ

**Abstract — Introduction:** TASERs deliver electrical pulses that can temporarily incapacitate subjects. The goal of this paper is to analyze the distribution of currents in muscle layers and understand the electro-muscular incapacitation safety and efficacy of TASERs.

**Methods and Results:** The analyses describe skeletal muscle and motor nerve activation, cell electroporation and current and electric field distributions through skin, fat and muscle layers, under worst-case assumptions for TASER electrode penetration and separation. For the muscle layer, the analysis predicts worst-case current-density and field-strength values of 94 mA/cm<sup>2</sup> and 47 V/cm. Both values are higher than thresholds required for neuromuscular activation but significantly lower than levels needed for permanent cellular electroporation or tissue damage.

**Conclusion:** The results indicate that TASERs are safe and effective in producing temporary subject incapacitation.

**Keywords —** Activation, Modeling, Muscle, Nerve, TASER.

## I. INTRODUCTION

TASERs deliver trains of brief, high-voltage but low-charge electrical pulses designed to temporarily incapacitate subjects through strong neuromuscular activation. They are used as non-lethal weapons by law enforcement personnel to subdue suspects. TASER devices utilize compressed nitrogen to project two small probes up to various ranges of 15, 21, 25 or 35 feet at a speed of over 160 feet per second [1].

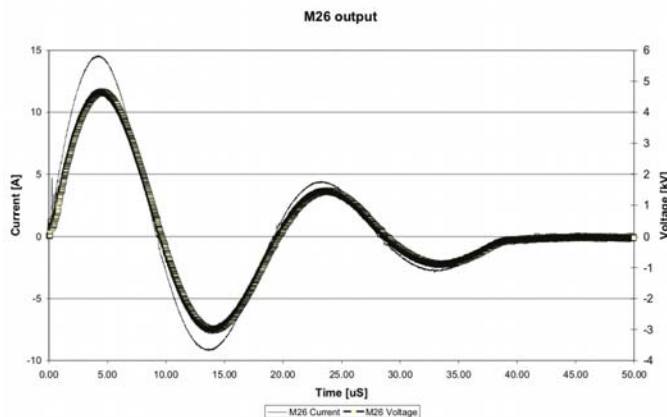


Fig. 1. M26 output for a 400-Ω load.

An electrical signal is transmitted through trailing wires to where the probes make contact with the body or clothing, resulting in an immediate loss of the person's neuromuscular control, with the initial reaction being a

gravitational dysreflexia (i.e. fall to the ground), and loss of ability to perform coordinated action for the duration of the impulse. The method of incapacitation is through electrical activation of skeletal muscle tissue innervated by peripheral nerves within the electric field created by the TASER device [1]. The stimuli from a TASER will override the motor nervous system and block the command and control of the human body. Conventional stun devices stimulate sensory neurons for pain compliance and can be overridden by a focused individual. The TASER devices directly stimulate pre-endplate motor nerve tissue, causing incapacitation regardless of subject's mental focus, training, size, or drug induced dementia [1]. The most popular TASER models supplied to law enforcement agencies are the M26 and X26. Their typical output waveforms are shown in Figs. 1 and 2, respectively.

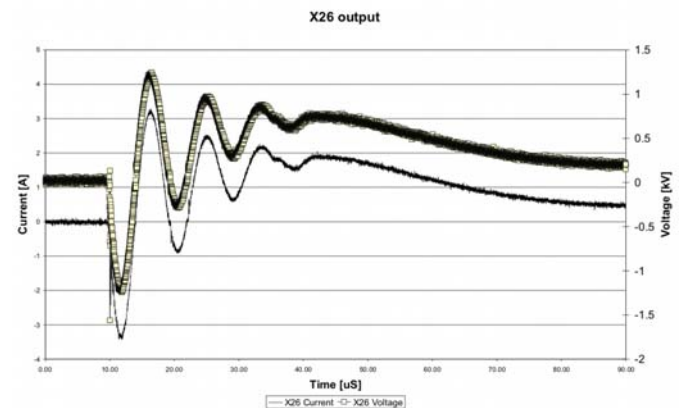


Fig. 2. X26 output for a 400-Ω load.

Table I provides a specification summary for these two devices. The goal of this paper is to analyze the distribution of currents in muscle layers and understand the electro-muscular incapacitation safety and efficacy of TASERs.

Table I. Specifications of M26 and X26 TASERs.

| Specification                              | M26  | X26  |
|--|------|------|
| Open-circuit peak voltage [kV]             | 50   | 50   |
| Output voltage in typical load [kV]        | 5    | 1.2  |
| Rated stored energy [J/pulse]              | 1.76 | 0.36 |
| Energy delivered in typical load [J/pulse] | 0.5  | 0.07 |
| Nominal internal power rating [W]          | 26   | 7    |
| Power delivered in typical load [W]        | 10   | 1.3  |
| Charge in the main phase [μC]              | 85   | 100  |
| Pulse rate [pulse/s]                       | 19   | 19   |
| Total delivery duration [s]                | 5    | 5    |

The M26 delivers a leading biphasic pulse pair of about 10- $\mu$ s duration for each half-cycle. The X26 delivers waveform that to a first approximation appears as a pseudo monophasic (half sinusoid) pulse of about 70  $\mu$ s.

## II. METHODS

The models analyzed herein describe skeletal muscle and motor nerve activation, cell electroporation and current and electric field distributions.

### A. Skeletal muscle activation by pulsed electric fields

In general, skeletal muscle activation by electrical stimulation is elicited by excitation of  $\alpha$ -motor neurons which innervate such muscle fibers. This fact often comes as a surprise, in that skeletal muscle cells are themselves excitable. Skeletal muscle excitability, however, is less than that of motor neuron cells in that both rheobase and chronaxie values of skeletal muscle are higher than those of the myelinated nerve axons which innervate them. Therefore, immediately adjacent to TASER dart locations it is possible that skeletal muscle fibers might be “directly” stimulated but any significant distance away from the darts one would expect skeletal muscle to be “indirectly” activated through its nervous innervation. Sensations of pain in response to TASER stimuli would be expected to result from a host of sensory nerve fiber types, to some extent dependent upon the specific locations of TASER dart attachment to the body (as well as the specific tissues located between and near the darts in what might be called the “capture” zone of the darts where excitable cells are activated). To elicit muscle activation then, each TASER pulse has to inject current through darts such that the electric fields created in the body capture sufficient volume of skeletal muscle, through indirect stimulation via motor nerves. At the same time, to avoid direct tissue damage, the current densities (J) and electric field strengths (E) have to be lower than, for example, thresholds that may produce cell electroporation. Based on existing modeling and experimental literature, we have assumed the following J and E thresholds for excitation:

- Motor neurons: chronaxie  $\sim$  140  $\mu$ s, rheobase E field  $\sim$  0.06 to 0.15 V/cm for excitation at axon terminations such as motor end-plates [4];
- Strength-duration correction of needed E field strength for the M26:  $(1 + 140/10) \times (0.06 \text{ to } 0.15 \text{ V/cm}) = 0.9 \text{ to } 2.25 \text{ V/cm}$
- Strength-duration correction of needed E field strength for the X26:  $(1 + 140/70) \times (0.06 \text{ to } 0.15 \text{ V/cm}) = 0.18 \text{ to } 0.45 \text{ V/cm}$

By comparison to these expected field strength values needed for neuromuscular activation, Gehl et al. have reported that for reversible and irreversible electroporation field strengths of 450 V/cm and 1600 V/cm are needed, respectively [5].

Based on these values, it is estimated that the E field required to successfully activate motor nerves with the M26 and X26 has to exceed 0.18-2.25 V/cm, whereas to avoid

electroporation E has to be less than 450-1600 V/cm. This yields a worst-case range for the E field strength of 2.25-450 V/cm, to insure successful activation with either device while also avoiding electroporation.

### B. FE modeling of J and E distributions

To understand the J and E distributions generated by TASER electrodes, we introduce a FE model with the following characteristics:

- Regions:
  - > Epidermis – 3 mm
  - > Dermis – 6 mm
  - > Fat – 5 mm
  - > Muscle – 6 mm
  - > Electrodes – 9-mm long, 2-mm diameter
- Nodes: 45360
- Elements: 41080 hexahedral elements
- Model: 15-cm long, 5-cm wide, 2-cm deep
- Dart electrodes 10-cm apart
- Voltage boundary conditions: 1000 V
- Steady-state solution

The FEM models the electrodes based on dimensions provided in [2, 3] and considers them fully penetrated. The inter-electrode distance is at the minimal end of reported actual-use separations [1-3]. The FE material properties are as reported in the literature [6]:

- Epidermis – 1 M $\Omega$ ·cm
- Dermis – 500  $\Omega$ ·cm
- Fat – 2200  $\Omega$ ·cm
- Muscle - 500  $\Omega$ ·cm
- Dart electrodes – 0.001  $\Omega$ ·cm

Note that the thickness of the fat layer is also at the low end of reported values. Additionally, the muscle layer is considered isotropic. If its anisotropy were included in the model, that would in fact only decrease the J and E magnitudes in this layer. Therefore, the conditions above represent a worst-case scenario for J and E distributions in the muscle layer. Actual-use values would not be expected to exceed the FEA prediction results.

## III. RESULTS

Figure 3 shows an example mesh of the FEM, its regions, as well as the overall current density distribution.

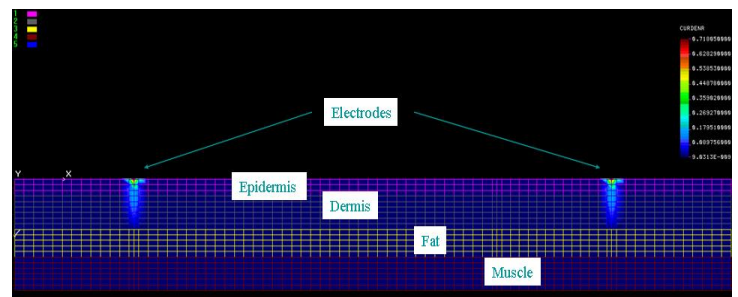


Fig. 3. FEM mesh and overall current density distribution.

The magnitude of  $J$  is listed in  $A/mm^2$ . Figure 4 presents a close-up of the current density values in the layers proximal to and under the electrode for the sample mesh. These layers are exposed to higher  $J$  and  $E$  values.

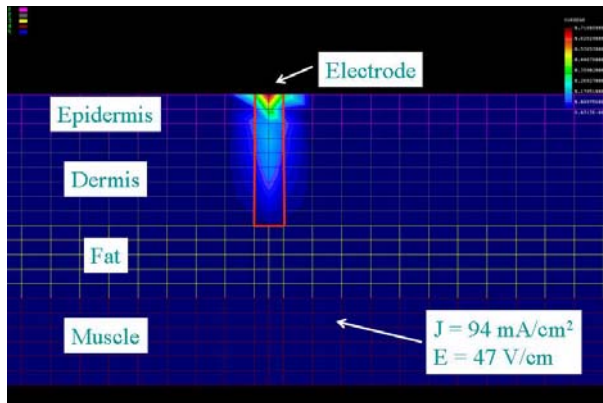


Fig. 4. FEM current density distribution.

As shown in Fig. 4, the highest  $J$  and  $E$  seen in the muscle layer, where the nerve density is presumably higher than in other layers, are  $94 \text{ mA/cm}^2$  and  $47 \text{ V/cm}$ , respectively. Note that  $J$  decreases dramatically 2-mm away from the electrode.

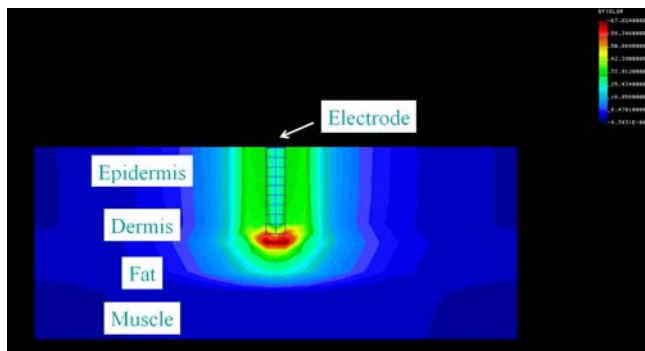


Fig. 5. FEM electric field strength distribution.

Figure 5 shows the distribution of  $E$  in a transversal cross-section through the center of an electrode. The values are expressed in  $V/mm$ . The electrode-electrode line is perpendicular to the plane of this section. The maximum  $E$  values are reached within a region, with a volume of approximately  $4 \text{ mm}^3$ , located about 1 mm beneath the electrode. While these values are somewhat higher than  $450 \text{ V/cm}$ , the threshold for reversible electroporation, they are far lower than  $1600 \text{ V/cm}$ , the threshold required for irreversible electroporation [5]. The magnitude of  $E$  also decreases rapidly with distance from the electrode, dropping below the threshold for reversible electroporation within a space less than 2 mm away from electrodes. Note that the  $E$  magnitude at the interface between the fat and muscle layers decreases quickly and reaches its overall model minimum, of about  $47 \text{ V/cm}$ , within a depth less than 1 mm. The values of  $E$  in the muscle layer, although more than 14 times lower than the  $E$  maximum, are still

greater by a significant margin than  $2.25 \text{ V/cm}$ , the threshold required to capture the motor neurons responsible for muscle activation.

#### IV. CONCLUSIONS

The analyses above, conducted for a worst-case scenario, predict  $J$  and  $E$  values for the muscle region higher than neuromuscular activation thresholds by a significant margin. Similarly, the predicted worst-case maximum values for  $J$  and  $E$  are lower, by at least a factor of two, than levels reported to produce permanent cellular electroporation or tissue damage. This safety margin would have been even higher had our models accounted for a nominal thickness of the fat layer and for the electrical anisotropy of the skeletal muscle. Therefore, we conclude that TASERS are efficient and safe in producing neuromuscular activation for temporary suspect incapacitation.

#### V. REFERENCES

- [1] TASER International: *TASER Technology Summary*. Available at <http://www.taser.com/facts/qa.htm>
- [2] TASER International, *Advanced TASER: M-Series Operating Manual*. 2005.
- [3] TASER International, *Advanced TASER: X-Series Operating Manual*. 2005.
- [4] J.P. Reilly, V.T. Freeman, and W.D. Larkin, "Sensory effects of transient electrical stimulation: Evaluation with a neuroelectric model," *IEEE Trans. Biomed. Eng.*, vol. 32(12), pp: 1001-1011, 1985.
- [5] J. Gehl, T.H. Sorensen, K. Nielsen, P. Raskmark, S.L. Nielsen, T. Skovsgaard, and L.M. Mir, "In vivo electroporation of skeletal muscle: threshold, efficacy and relation to electric field distribution," *BBA-General Subjects.*, vol. 1428(2-3), pp. 233-20, 1999.
- [6] D. Panescu, J. G. Webster and R. A. Stratbucker, "A nonlinear finite element model of the electrode-electrolyte-skin system," *IEEE Trans. Biomed. Eng.*, vol. 41, no. 7, pp. 681-687, 1994.